Case Studies in Thermal Engineering 39 (2022) 102391

Contents lists available at ScienceDirect

Case Studies in Thermal Engineering

journal homepage: www.elsevier.com/locate/csite

Prediction of heat transfer coefficient, pressure drop, and overall cost of double-pipe heat exchangers using the artificial neural network

Andaç Batur Çolak [a,*], Özgen Açıkgöz [b], Hatice Mercan [c], Ahmet Selim Dalkılıç [b], Somchai Wongwises [d,e]

[a] Department of Mechanical Engineering, Engineering Faculty, Niğde Ömer Halisdemir University, Niğde, 51240, Turkey
[b] Department of Mechanical Engineering, Mechanical Engineering Faculty, Yildiz Technical University (YTU), Istanbul, 34349, Turkey
[c] Department of Mechatronics Engineering, Mechanical Engineering Faculty, Yildiz Technical University (YTU), Istanbul, 34349, Turkey
[d] Department of Mechanical Engineering, Faculty of Engineering, King Mongkut's University of Technology Thonburi (KMUTT), Bangmod, Bangkok, 10140, Thailand
[e] National Science and Technology Development Agency (NSTDA), Pathum, Thani, 12120, Thailand

ARTICLE INFO

Keywords:
Artificial neural network
Multi-layer perceptron
Levenberg-Marquardt
Optimum velocity
Double-pipe heat exchanger

ABSTRACT

Typically, success in the estimation of machine learning is expected to rise with increasing input parameters, whereas the noise issue may rarely arise owing to redundant input factors undesirably influencing the learning algorithm. The parameters such as overall heat transfer coefficient, pressure drop, and overall cost have been determined by two different artificial neural networks evaluated by a multi-layer perceptron model. Using the Levenberg-Marquardt training algorithm, in the first model input layer, a total of 10 input parameters ρ, n_p, k_1, Re_1, f_i, Re_2, f_o, n_s, P_1 and P_2 have been defined, while the second involves 8 input parameters by subtracting pumping powers from the first one, thus the noise issue has been investigated using unnecessary input parameters. Overall heat transfer coefficient, tube/annulus sides pressure drops, and overall cost have been estimated with deviations of 0.16%, 0.23%, 0.02%, and 0.003% via Model 1, 0.02%, 0.18%, 0.16%, and 0.15% via Model 2, respectively. Moreover, Model 1 results in the best mean squared errors for annulus side pressure drop and overall cost with the values of 2.54E-04 and 1.93E-04, correspondingly, whereas Model 2 yields the best values of 1.11E-04 and 1.90E-04 for overall heat transfer coefficient and tube side pressure drop, sequentially.

Nomenclature

A	inner surface area, m^2
ANN	artificial neural network
C	pipe element price, USD
COP	coefficient of performance
CFD	computational fluid dynamics
c_p	specific heat, J $kg^{-1}K^{-1}$

* Corresponding author. Department of Mechanical Engineering, Engineering Faculty, Niğde Ömer Halisdemir University, Niğde, 51240, Turkey.
E-mail address: andacbaturcolak@hotmail.com (A.B. Çolak).

https://doi.org/10.1016/j.csite.2022.102391
Received 3 May 2022; Received in revised form 15 August 2022; Accepted 27 August 2022
Available online 2 September 2022

d	diameter, m
f	friction factor
h	convective heat transfer coefficient, W $m^{-2}K^{-1}$
HEX	heat exchanger
HT	heat transfer
HTC	heat transfer coefficient, W $m^{-2}K^{-1}$
k	thermal conductivity, W $m^{-1}K^{-1}$
L	tube length, m
$\dot{m}$	mass flow rate, kg s^{-1}
MLP	multi-layer perceptron
MSE	mean squared error
n	number of pipes
Nu	Nusselt number
P	pumping power, W
Pr	Prandtl number
R	coefficient of determination
$\dot{Q}$	heat transfer rate, W
R_f	fouling factor, m^2 K W^{-1}
Re	Reynolds number
T	temperature, °C
t_m	average temperature, °C
U	overall heat transfer coefficient, W $m^{-2}K^{-1}$
X	variable
w	flow velocity, m s^{-1}
ΔP	pressure drop, Pa
ΔT	temperature difference, K

Greek symbols

η	efficiency, %
θ_y	amortization period, year
θ_h	operating period, hour
μ	dynamic viscosity, Pa.s
ν	kinematic viscosity, m^2 s^{-1}
ρ	density, kg m^{-3}
φ	particle concentration

Subscripts

el	electric
exp	experimental
f	fluid
F	fouling
h	hydraulic
i	inside
in	inlet
lm	logarithmic
m	mean
o	outside
out	outlet
p	parallel
pred	predicted
s	series
sum	sum
1	tube side
2	annulus side

1. Introduction

Heat exchangers (HEXs) have commonly benefitted industrial and domestic systems for instance, refrigeration and HVAC, vehicles, power cycles, and production plants. The complication in evaluating them is due to their technical types and the physical occurrences

taking place during the heat transfer (HT) between the liquid or gas mediums. In most cases, they have been studied numerically, analytically, and experimentally in light of the principles of thermodynamics. Their theoretical examinations include more assumptions and complex equalities; on the other hand, practical approaches are pricey owing to the first investment necessary for establishing an experimental apparatus. To address these problematic points, artificial neural networks (ANN) have been generated for simulation, optimization, and estimation of thermal applications having HEXs.

The appropriate choice of a HEX is a difficult task for engineers. Primarily, the noteworthy factor is to acquire thermal load precisely. Afterward, other ones are working pressure, flow rate, and chemical compatibility requirements. In addition to heat transfer (HT), these elements comprise the arrangement and substance. The prediction and operation of optimum velocity are two of the ignored items of HEX design issues that have a key position in the choice of the instrument concerning first and operative expenses. The mean flow velocity in HEXs is rarely evaluated, and hence requires additional and thorough research due to its critical influence on the total thermal performance of the system. That is to say, tube diameter is a remarkable input in the HT fundamentals encompassing examination of expenditures. The essential target of this work is to recall the effect of several types of pure fluids and their nanoparticle-added states on the optimum velocity impacting HT fundamentals, pumping power, and total cost, and to reveal the most appropriate and economic nanofluid for HEXs. The key goal of the present investigation is to model several fluids with added nanoparticles passing through the pipe side of the double pipe HEX using the procedures of MLP and NLS as beneficial tools of ANN structures employing various parametric estimation data. In the following paragraphs, we mention some of the latest numerical investigations related to machine learning methods including ANN analysis.

ANN derives equations depending on training data that necessitate no definite analytical equalities or application properties. Nonlinear factors related to the HT practices of HEXs may be derived as a correlation by applying ANN analyses with low deviations [1]. Thermal investigations of HEXs utilizing ANN have recently been commonly performed. ANN is becoming popular as a numerical solution method that is successfully applied for the analysis of the HT characteristics of HEXs under admissible accuracy. According to a review paper by Mohanraj et al. [1], works on the subject can be classified into four main categories: the modeling of HEXs, the prediction HEX factors, the characteristics of phase change prediction, and the control of HEXs. In their study, the restrictions of ANN usage and the upcoming investigation required on the subject have been revealed. Recently published articles regarding ANN efforts for defining the HT characteristics of HEXs are summarized as follows:

Devi et al. [2] used the plain swirl tape improvement method that is most prevalently utilized in the application of air conditioning and air refrigeration systems. They aimed to obtain the Nusselt number (*Nu*) of a double-pipe HEX with this passive improvement technique having various swirl ratios, both experimentally and numerically. Their work focused on the most utilized approximation named MLP-ANN having a 3-layer feed-forward neural network applied to find the *Nu*. Their numerical model's inputs were the Prandtl number (Pr), twist ratios, and Reynolds number (Re), and they obtained 33 experimental data that were evaluated for training. Numerical outputs indicated that the *Nu* determined by the studied MLP-ANN model has a high accuracy and a very low error rate in the prediction of the *Nu*.

Sharifi et al. [3] emphasized the difficulties of the development of a new correlation for a sophisticated thermal application having passive HT enhancement techniques. Their numerical model was a combination of computational fluid dynamics, ANN, and a genetic algorithm. For this purpose, they first obtained a 3D computational solution for fluid flow data using the computational fluid dynamics (CFD) technique. After verification of the CFD model, they examined the wire coil inserted pipes via the verified model to find the heat transfer coefficients (HTCs) and friction factors. Afterward, they selected a comprehensive ANN algorithm for testing the heat exchangers. In conclusion, to find which kind of heat-exchangers operate more desirably, they employed the optimization method of the GA together with the ANN simulation. Outputs disclosing the state of the most suitable helical wire type was determined according to HT efficiency values. Researchers also indicated that the improper selection of wire inserts can reduce the efficiency of the heat exchanger unexpectedly.

Moya-Rico et al. [4] suggested a numerical model for ANNs predicting HT characteristics in a triple concentric-tube HEX with smooth and enhanced surfaces that include corrugation with various pitch and depth values. They accomplished their ANN simulation by evaluating 181 practical data points. According to their analyses, the most proper training option is the Bayesian regulation. They examined various ANN configurations, and consequently concluded that the optimum one includes a configuration having two hidden layers with 15 and 21 neurons in the first and second layers, in turn. The numerical outputs have been successful in the prediction of practical data, whose absolute mean relative error band is less than 1.91% for the HTC and 3.82% for the pressure drop (PD), in turn.

Verma et al. [5] aimed to determine the HT performance of a suggested 2 m length and 25.4 mm diameter manufactured HEX with varied corrugated and smooth tubes. Researchers focused on the details of corrugation to accomplish the maximum HTC and *Nu*. An ANN algorithm for estimating HTC, *Nu*, and Re was developed with an optimized structure of ANN at 8-10-3. Finally, they calculated R^2 values calculated as 0.99999 for all investigated outputs.

Hojjat [6] generated an ANN to determine the thermal and hydrodynamic characteristics in a shell and tube HEX. Nanoparticle volumetric proportion, Re, thermal conductivity, and Pr were the inputs, while *Nu* and PD were the outputs of their numerical model. They conducted multi-objective optimization to minimize the total PD and maximize the nanofluids' *Nu* in the HEX through a non-dominated sorting genetic algorithm structure. Outcomes reveal that the developed ANN structure can estimate the tested database with a maximum of 9% and 9.6% deviations for *Nu* and PD, respectively.

Taheri et al. [7] researched the alteration of the traditional heat sink, heat pipe structure to enhance HT performance. Their experimental model was based on the novel concept of a liquid-cooled heat sink with an MWCNT/water nanofluid for thermal control. Their criteria for the evaluation of tested sections include the PCB transient/steady temperature, the time necessary for reaching a steady-state regime, the mean thermal resistance of the cooling section, circuit cooling under discontinuing loads, and thermal performance. The radial-basis function and multi-layer perceptron (MLP) as ANN methods were beneficial in determining the steady-state

temperature of the PCB, applying a proposed cooling section for other working parameters. Consequently, at the maximum used heat flux, the highest energy efficiency is achieved at approximately 59.2% for the flow of MWCNT/water nanofluid having a mass concentration of 0.3%.

Naphon et al. [8] used CFD and ANN analyses to examine the nanofluids' jet impingement HT and hydrodynamic behavior in a microchannel heat sink. They accomplished this optimization study using the Levenberg-Marquardt backward propagation training structure and the Eulerian two-phase approach model for the ANN and CFD models, respectively. They performed a validation study through the comparison of ANN and CFD data with measured ones. In the ANN results, most of the data were in the deviation bands of ±1.5% for both the *Nu* and PD. They also calculated the largest error for all tests at 1.25%.

Davoudi and Vaferi [9] discussed the fouling problems that occur on HT surfaces and emphasized the inaccurate obtained results from practical studies due to the fouling issues of HEXs. The ANN method was suggested as a solution for estimating the fouling factor. Many data points have been evaluated for the improvement study of the ANN model. They enabled the minimization of the numerical struggle and maximization of statistical precision via the Bayesian regulation backpropagation method as the best training structure and optimum number of hidden neurons. They also predicted fouling factors from practical data and developed an ANN model with very high accuracy.

Duran et al. [10] aimed to create a model for an early design on cost prediction for shell and tube HEXs. They benefitted from the ANN technique for accurate estimations, even in cases with no necessary knowledge in the beginning phase of the design. Their results indicated that ANN analyses can reduce uncertainties regarding the predicted cost of a shell and tube HEX.

Some of the studies including passive HT enhancement techniques for HEXs are summarized as follows:

Noorbakhsh et al. [11] numerically researched the increase in HT in a double tube HEX with a twisted band as a vortex generator. They conducted three-dimensional numerical simulations using the finite volume method; they also obtained the spatial discretization of the mass, momentum, turbulent dispersion rate, and turbulent kinetic energy formulas with a quadratic upwind scheme. They also evaluated the Green-Gauss cell-based method to determine the gradients, and they considered the vortex generator in both channels of the HEX. Three different types of nanofluids containing Al_2O_3, CuO, and SiO_2 were accepted as the HT fluid in the inner channel. The outcome indicated that the highest thermal performance pertains to the CuO/water nanofluid, which has a 7% increase in thermal performance in comparison to water.

Karouei et al. [12] proposed a helical twin-pipe HEX with a finned, semi-conical section and an advanced turbulator with two holes inside. They considered two geometric parameters in the model, namely the angle of the tabulator blades and the number of tabulator blades. The results first showed that the best thermal stratification can be obtained at the fin angle of 180°, and the lowest mass flow rate studied, the HTC of the turbulator with the fin angle of 180°, is higher than the case without the turbulator.

Noorbakhsh et al. [13] numerically investigated the impact of employing twisted bands with several geometries on both pipes of a double tube HEX. They considered cases in which the fluid is water on both sides of the double-pipe HEX discussed in the study. They numerically analyzed the effect of geometric parameters such as the number of twisted strips and gap formation on the twisted strip with dissimilar aspect ratios. They calculated and evaluated the outlet temperature, pressure drop, *Nu*, and coefficient of performance (COP) for both sides. Their findings showed that increasing the number of twisted bands from a single blade to four blades resulted in a 3.1% increase in the *Nu*, a 64% increase in pressure drop, and a 63.9% rise in the COP.

Karouei et al. [14] numerically investigated the influence of placing an advanced curved turbulator and using two sorts of hybrid nanofluids on thermal performance in a helical twin-tube HEX. They used silver, graphene, and multi-walled carbon nanotube-iron oxide as nanoparticles, with water preferred as the base fluid. The studied novel turbulator has 12 blades to generate secondary flows, and a hole at the tip of the turbulator is assumed. The results of the study showed that using this proposed progressing turbulator causes a higher HT rate and that a silver-graphene/water hybrid nanofluid improves thermal performance at a low mass flow rate.

Karouei and Ajarostaghi [15] numerically investigated HT and fluid flow in a dual coil HEX with a new vortex generator with a curved inner channel. The turbulator under consideration consists of a coiled structure and 12 blades to make up swirl flows, and two holes have been formed in the semi-conical section of the turbulator. They investigated the influences of the geometric factors of the suggested turbulator, involving the radius of the turbulator and its holes. The results showed that the highest efficiency corresponds to the situation where the diameter of the turbulator and the radius of the turbulator holes are equivalent to 19 and 3.6 mm, correspondingly. In addition, swirl flows created by the turbulator were stated to have a significant effect on HT improvement.

In this paragraph, we briefly discuss some of the works related to machine learning methods excluding ANN analysis. In his study, Sridharan [16] used a basic numerical way to estimate the efficiency of a concentric HEX employing fuzzy logic that included two fuzzy interference structures as Mamdani and Sugeno. For this purpose, he obtained 48 sets of practical data under different mass flow rates of hot and cold fluids. According to the comparison of practical and estimated outputs, Sugeno-based numerical models were noticed to be more predictive than Mamdani-based ones. Some of the recently performed investigations based on ANN analyses of HEXs have focused on finding the following: techniques of fouling in HEXs in food production [17]; computational work on hydrothermal attributes of a nanofluid in a spiral HEX [18]; nanofluids in the shell and tube cooling HEXs of gasoline material of the residual fluid catalytic cracking unit [19]; optimization of ground-source HEXs for buildings employing the Taguchi technique [20]; modeling of a helically corrugated coiled tube-in-tube HEX [21]; optimization of helical micro fin pipes depending on exergy destruction minimization [22]; energy and exergy analyses for the impact of the finned coiled wire insert in a circular tube [23]; optimization of a double-pipe HEX having nanofluids by ANFIS; and ANN modeling [24] and determination of the HTCs of shell and coiled tube HEXs benefitting from computational and experimental techniques [25]. The abovementioned investigations of HEXs and industrial and domestic uses of ANN verified that no specific work exists on the handling of ANN for the determination of optimum velocity in a HEX. Therefore, this numerical investigation should be a model for future studies and should fill the gap in open sources. It can be noted that the present paper should be assessed as a follow-up to the authors' recently published investigations [26,27]. The primary purpose of

the current research should be seen as modeling the single-phase pure and nanofluid flows in a double-pipe HEX in MATLAB by the techniques of MLP and NLS, and then evaluating the most influenced factors and generating reliable equations with several groups of optimum data for velocity determination [26,27]. The suggested model is thought to help estimate some HEX design parameters of other configurations without additional parametric work, owing to the usage of reliable data from the authors' previous publications [26,27].

2. Parametric calculation procedure

2.1. Thermophysical properties

The used inputs from the numerical models do not include any parameters specifically calculated for nanofluids flowing in the tube side; in other words, the database has not been divided into any groups, they have been used as whole groups during ANN analyses. To enable content integrity, the procedure for the calculation of thermophysical specifications of nanofluids can be gained from the authors' former studies [26,27].

2.2. Heat transfer analysis

The parametric model methodology has been given between Eqs. (1) and (6) and are valid for the pipe side of the multi-double pipe HEX (hairpin type). The HT rate from the hot fluid is determined in Eq. (1).

$$\dot{Q} = \dot{m}_1 c_{p,1}\left(T_{1,in} - T_{1,out}\right) \tag{1}$$

The number of parallel tubes [28], velocity, and Re is found using Eqs. (2)–(4) respectively.

$$n_p = \frac{\dot{m}_1}{\frac{\pi d_i^2}{4} w_1 \rho_1} \tag{2}$$

$$w_1 = \frac{\dot{m}_1}{\frac{\pi d_i^2}{4} n_p \rho_1} \tag{3}$$

$$Re_1 = \frac{w_1 d_{1,i}}{\nu_1} \tag{4}$$

Convective HTC is obtained using Eq. (5) for non-boiling water during turbulent flow ($10<d_i<100$ mm and $L>1000$ mm) [29],

$$h_1 = 3373(1 + 0.0014 t_m) {w_1}^{0.85} \tag{5}$$

where the average temperature is acquired using Eq. (6).

$$t_m = \frac{T_{1,in} + T_{1,out}}{2} \tag{6}$$

The formulas from Eqs. (7)–(17) are valid for the annulus side of the investigated HEX. Re, velocity, and hydraulic diameter are found in Eqs. (7)–(9), in turn.

$$Re_2 = \frac{w_2 d_{2,h}}{\nu_2} \tag{7}$$

$$w_2 = \frac{\dot{m}_2}{\frac{\pi\left[\left(d_{2,i}\right)^2 - \left(d_{2,o}\right)^2\right]}{4} n_p \rho_2} \tag{8}$$

$$d_{2,h} = \frac{4\left[\left(\frac{\pi d_{2,i}^2}{4}\right) - \left(\frac{\pi d_{1,o}^2}{4}\right)\right]}{\pi d_{2,i} + \pi d_{1,o}} = d_{2,i} - d_{1,o} \tag{9}$$

In round tubes and for laminar flow, the Nu is obtained using Eq. (10) as proposed by Hausen [30]. Accordingly, Gnielinski [31]'s Nu is given in Eq. (11) for the turbulent flow in round tubes,

$$Nu_2 = 3.66 + \frac{0.19\left(Re_2 Pr_2 \frac{d_{2,h}}{L}\right)^{0.8}}{1 + 0.117\left(Re_2 Pr_2 \frac{d_{2,h}}{L}\right)^{0.467}} \qquad 0.1 < Re_2 Pr_2 \frac{d_{2,h}}{L} < 10^4 \tag{10}$$

$$Nu_2 = \frac{\left(\frac{f_2}{2}\right)(Re_2 - 1000) Pr_2}{1 + 12.7\left(\frac{f_2}{2}\right)^{\frac{1}{2}}\left(Pr_2^{\frac{2}{3}} - 1\right)} \tag{11}$$

where Eqs. (7) and (12) give Re and friction factor, correspondingly.

$$f_2 = (1.58 \ln Re_2 - 3.28)^{-2} \tag{12}$$

Convective HTC, overall HTC, and logarithmic temperature difference are determined using Eqs. (13)–(15), in that order,

$$h_2 = Nu_2 \frac{k_2}{d_{2,h}} \tag{13}$$

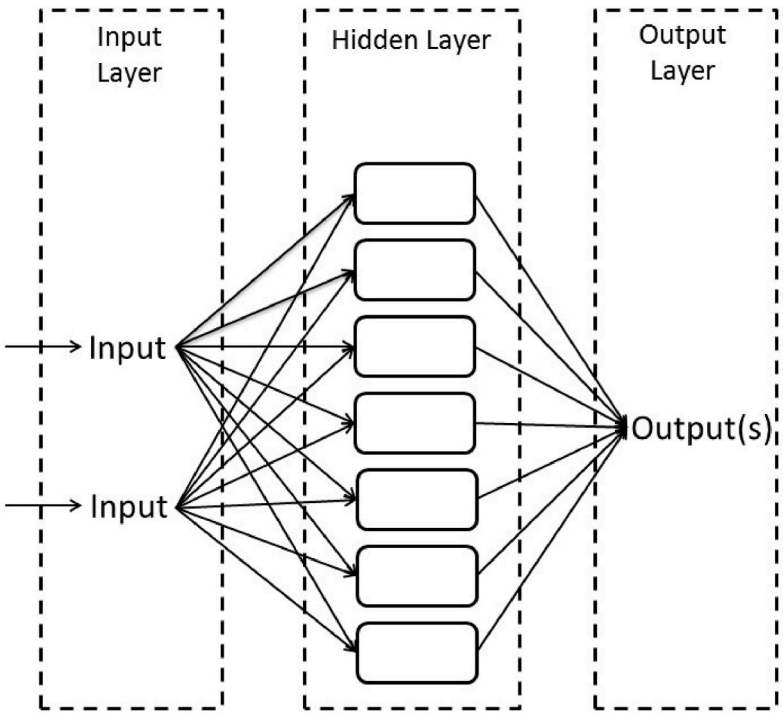

a)

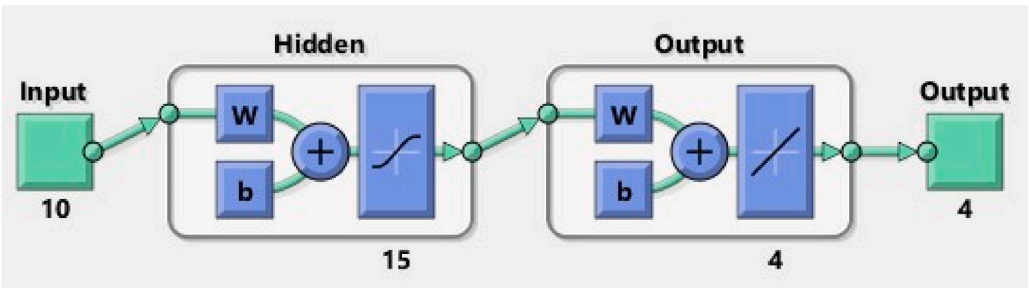

b)

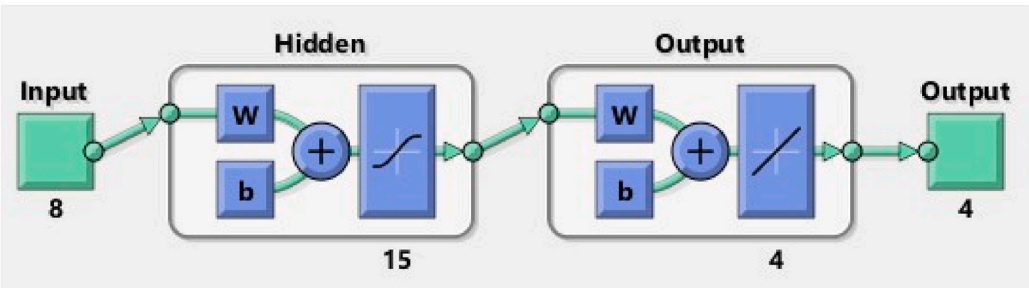

c)

Fig. 1. The schematic structure of an MLP network (a), the network structures of two different ANN models developed (b, c).

$$\frac{1}{U_o}=\frac{1}{h_1}\frac{A_2}{A_1}+R_{F,1}\frac{A_2}{A_1}+\frac{\ln\left(\frac{r_2}{r_1}\right)}{2Lk_1}A_2+R_{F,2}+\frac{1}{h_2} \tag{14}$$

where fouling factors are taken as 0.0001 m^2K/W.

$$\Delta T_{lm}=\frac{\Delta T_1-\Delta T_2}{\ln\left(\frac{\Delta T_1}{\Delta T_2}\right)} \tag{15}$$

To compute the total heat transfer area of the HEX, Eq. (16) is used and the total pipe number is gained using Eq. (17).

$$A_o=\frac{\dot{Q}}{U_o\ \Delta T_{lm}} \tag{16}$$

$$n=\ n_s n_p=\frac{A_0}{\pi d_{1,0}L} \tag{17}$$

2.3. *Pressure drop analysis*

Eq. (18) is for the tube side, while Eqs. (19) and (20) are for the annulus side [32]. It should be noted that the *m* value is assumed for laminar and turbulent flows as 0.25 and 0.14, respectively [32],

$$\Delta P_1=n_s\left[f_i\frac{L}{d_{1,i}}\left(\frac{\mu}{\mu_1}\right)^{-m}+2.5\right]\frac{\rho_1 w_1^2}{2} \tag{18}$$

$$\Delta P_2=\ n_s\left[f_o\frac{L}{d_{2,h}}\left(\frac{\mu}{\mu_2}\right)^{-m}+2.5\right]\frac{\rho_2 {w_2}^2}{2} \tag{19}$$

where the hydraulic diameter is determined by Eq. (20) and the friction factor [33] is calculated from Eq. (21) for $Re < 2300$, Eq. (22) for $2300 < Re < 20000$ and Eq. (23) for $Re > 20000$.

$$d_{2,h}=\frac{\pi\left(d_{2,i}^2-d_{1,o}^2\right)}{d_{1,o}} \tag{20}$$

$$f=\frac{64}{Re} \tag{21}$$

$$f=\frac{0.3164}{Re^{0.25}} \tag{22}$$

$$f=\frac{0.184}{Re^{0.2}} \tag{23}$$

2.4. *Cost analysis*

The pumping power is calculated by Eq. (24) for both sides of the HEX taking pump efficiency as 70% individually.

$$P=\frac{\dot{m}\ \Delta P}{\rho\ \ \eta} \tag{24}$$

Annual investment, working, and overall costs [28] are obtained using Eqs. (30)–(32), respectively.

3. ANN development

To estimate U_o, ΔP_1, ΔP_2, and C_{sum} values, we have designed two dissimilar MLP-ANN models. MLP algorithms are among the most frequently used ANN algorithms with their robust structures and high learning skills [34–36]. The first layer of MLP networks is the input layer in which the training data is introduced to the system. After the input layer, there is a hidden layer that contains the numerical parameter named in the neuron [37]. In the final layer, the output layer, the forecast values are obtained. The schematic structure of an MLP structure is illustrated in Fig. 1a. In the first model input layer, named Model 1, we have defined a total of 10 input parameters ρ, n_p, k_1, Re_1, f_i, Re_2, f_o, n_s, P_1 and P_2. In the second model, we have defined 8 input parameters by subtracting P_1 and P_2 parameters from the input parameter group. These are the leading factors for the determination of optimum velocity [26,27]. One of the significant parameters in the development of ANN models is the ideal optimization and grouping of the data set. While it may be possible to have an over-learning situation in ANN models developed with an excessive amount of data, the prediction performance of models developed with insufficient data may be low [38]. Therefore, the data set has been classified using the method with a high accuracy reported in the literature [39–41]. In the ANN model, designed using a total of 438 data sets, 306 of the data sets have been evaluated for training the model, 66 for validation, and 66 for testing. Determining the algorithm to be evaluated in the training of the ANN structure is among the significant stages in the training performance of the model. ANN algorithms can be developed using

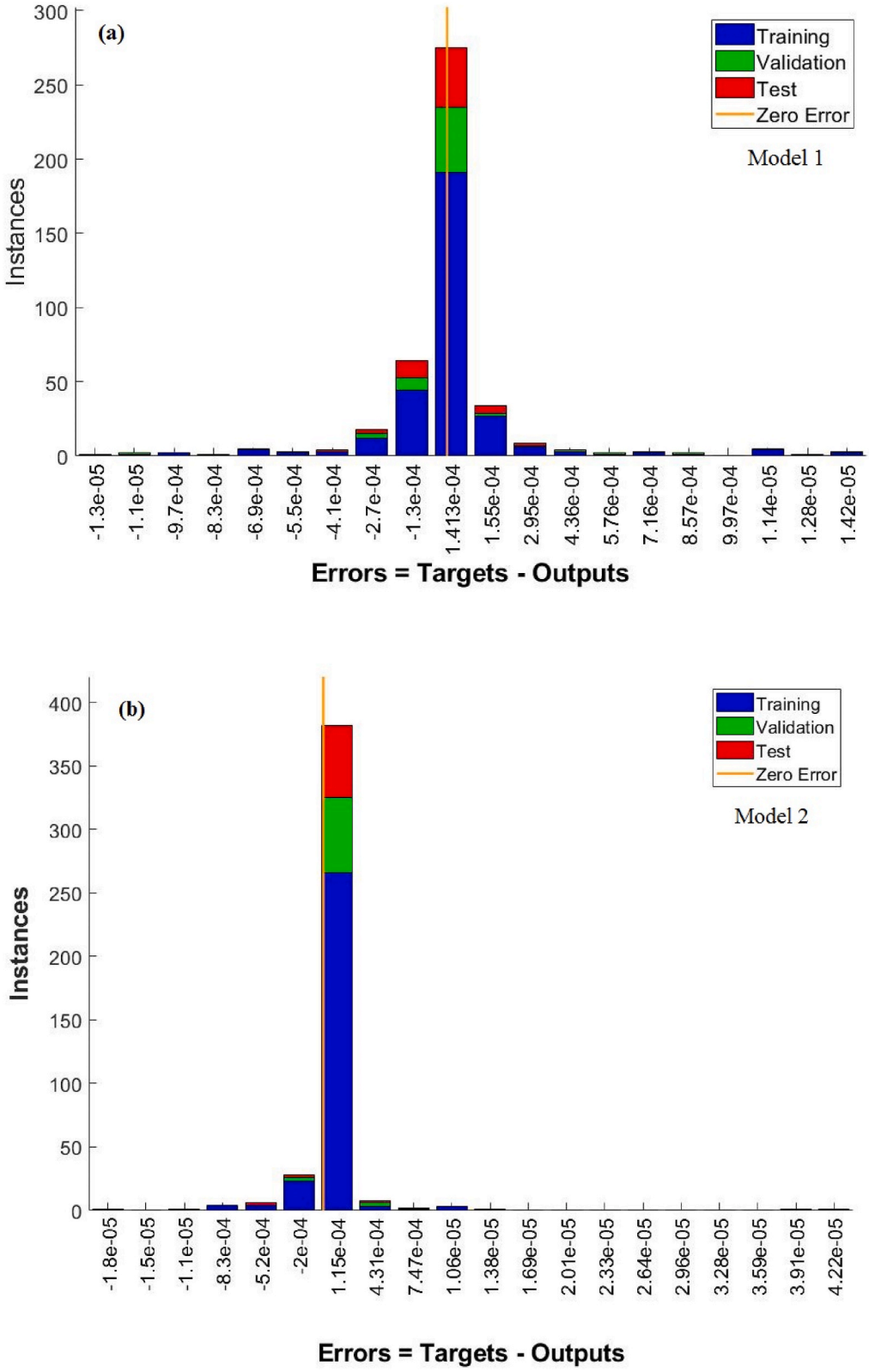

Fig. 2. Error histogram of the ANN models.

different training algorithms. There are some investigations on the performance analysis of training algorithms [42]. The Levenberg-Marquardt training algorithm, due to its strong functional feature, is one with a high training capability and that is frequently used in ANN models [43,44]. Considering all these advantages, we used the Levenberg-Marquardt training algorithm in the developed ANN model. Tan-Sig and Purelin transfer functions are used in the hidden and output layers of the MLP network, in turn. The transfer functions used are indicated below [45,46].

$$f(x) = \frac{1}{1 + \exp(-x)} \tag{29}$$

$$\text{purelin}(x) = x \tag{30}$$

One of the problems in the generation of ANN structures is to determine the number of neurons to be used in the hidden layer. There is no model or mathematical expression in use for calculating the number of neurons [47]. For this reason, as is done in the literature, we examined the performance of network models generated with several neuron numbers, and we obtained the maximum estimation performance from the model with 15 neurons in the hidden layer. The network structures of two different created ANN models are depicted in Fig. 1b. We calculated the mean squared error (MSE) and coefficient of determination (R), which are frequently used, to analyze the training and forecast performance of both ANN algorithms, and we evaluated the results. The proportional deviations between the outcomes gained from the ANN models and the target data have also been calculated and analyzed. The analytical expressions evaluated are given as [48]:

$$\text{MSE} = \frac{1}{N}\sum_{i=1}^{N}\left(X_{\text{targ(i)}} - X_{\text{pred(i)}}\right)^2 \tag{31}$$

$$R = \sqrt{1 - \frac{\sum_{i=1}^{N}\left(X_{\text{targ(i)}} - X_{\text{pred(i)}}\right)^2}{\sum_{i=1}^{N}\left(X_{\text{targ(i)}}\right)^2}} \tag{32}$$

$$\text{Deviation}\ (\%) = \left[\frac{X_{\text{targ}} - X_{\text{pred}}}{X_{\text{targ}}}\right] x\ \ 100 \tag{33}$$

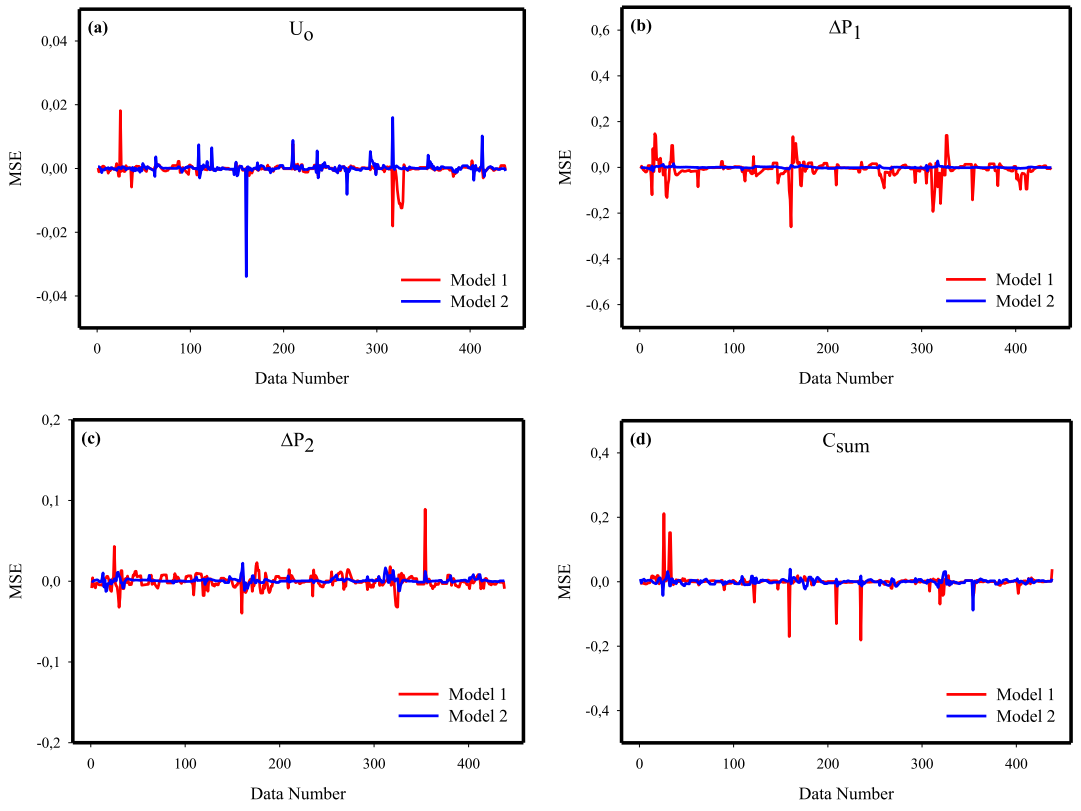

Fig. 3. MSE values for the developed ANN models.

4. Results and discussion

Tubing is among the most noteworthy subjects in the expenditure of industrial applications. It is a reality that 80% of the cost of tools or 20% of fixed assets may be due to the prices of piping in thermal systems. Tube diameter, and thus flow velocity, strongly influences the current value of the system in terms of electricity consumption, and the cost of fitting tubes, pumps, and valves. A sample model of the comprehensive expenditure method for various fluids with their pure and mixture versions with nanoparticles in liquid phase flowing in an inner pipe side of tube-in-tube HEX has been investigated. Pressure drop, in other words, or pumping power rises with increasing flow velocity, whereas overall expenditure illustrates a curve. The obvious result is that a minimum expenditure exists as a consequence of the parametric calculations for every tested fluid.

In the current numerical research, the 438 parametric datasets have been formed for the several fluids. It should be noted that water has been flowing on the annulus side while the other fluids have been flowing on the inner side. We have determined the proper economic working conditions based on the calculation of optimum velocity in the inner tube for the multi-double-pipe HEX (hairpin type) [26,27].

Artificial intelligence tools that can predict with high accuracy by learning even non-functional relationships between data are widely used in almost every field [49]. In the field of artificial intelligence, there are different tools such as ANNs, genetic algorithms, particle swarm optimization, fuzzy logic, simulated annealing, intelligent bee algorithm, and hybrid approaches [50]. ANNs, which have a very high prediction ability in comparison to traditional mathematical tools, are among the most commonly benefitting artificial intelligence methods [51]. The use of the ANN structure is preferred because of its advantages such as its strong structure and high learning ability in a great number of experimental data sets.

The initial step in the performance evaluation of ANN is to check their reliability in training. The error histogram depicting the error values obtained through the training stage, which was created for this purpose, is shown in Fig. 2. The main purpose of error histograms is to have an idea about the training accuracy of the ANN algorithm by analyzing the error values gained from the training stages. As the error histogram illustrated in Fig. 2 is reviewed, we observe that the error values calculated for the training, validation, and test data sets are placed around the zero error line. On the other hand, the computational values of the errors in the x-axis are quite small, as well. The outcomes acquired from the error histograms demonstrate that the training stages of both developed ANN models are finalized in a desired way with small errors.

In Fig. 3, the MSE values of both ANN models are given for each output parameter. Examination of MSE values is significant for the training and estimation validation of network models. There is a linear relationship between the proximity of the MSE values to zero and the prediction accuracy of the structure. As the MSE values found for each of the 438 data sets employed in the creation of the ANN

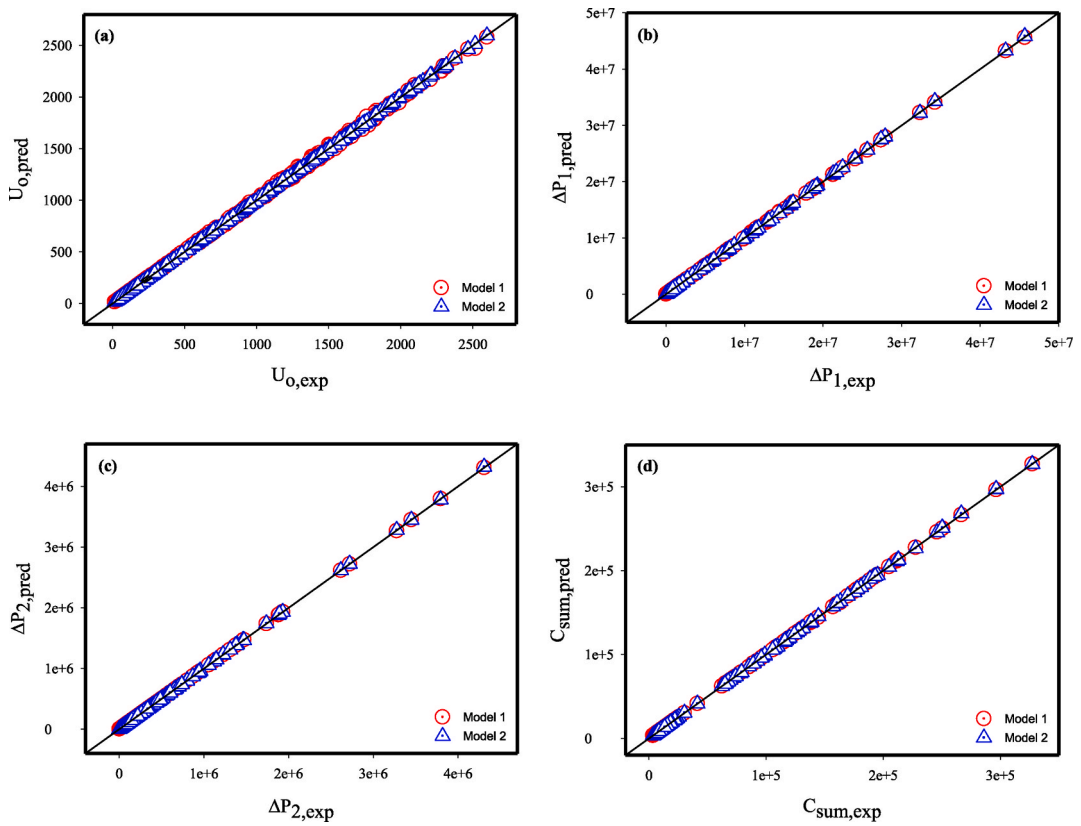

Fig. 4. The target and ANN outputs for both models.

models are reviewed, it is noticed that the MSE values obtained for both models are close to the zero line. It is seen that the MSE values calculated for each of the four different parameters are much lower than the MSE values obtained in similar studies in the literature [52]. These small values for MSE verify that both created ANN models have low errors and are trained to predict output parameters with low error values.

To examine the forecast accuracy of the ANN structures comprehensively, target and forecast data are displayed on the same graph to see the harmony between the data. In Fig. 4, the target data is on the x-axis, and the ANN model outputs are on the y-axis. When the situations of the data points are analyzed, all 438 data lie on the zero error line. The fact that the data obtained for both ANN structures are taking place on the zero error line indicates that both ANN structures have been developed to estimate output parameters with high precision.

As a consequence of the comprehensive examination of the data obtained because of the calculations made on the training and estimation performance of both developed ANN models, we can see that both network structures can be estimated with high precision. The determined R values for the created ANN models were above 0.98. The proximity of the R values to 1 is directly proportional to the high estimation precision of the ANN structure. In the investigations of ANN in the open sources, it is stated that R values calculated as 0.8 have satisfactory prediction performance [53]. The R values obtained for the ANN models proposed in this study have higher values compared to the values in the literature. These outcomes gained from the R values prove that the developed ANN models are ideally trained. As the deviation values determined for the proposed ANN models are analyzed, one can notice that generally very slight deviations are obtained. Thus, the maximum deviation is −0.23%. Considering the deviation values in the literature, we see that the deviations of 5% [54,55] and 6.98% [56] are considered ideal. Compared to these given studies, we see that the deviations obtained are much lower. By comparing the models generated by various input parameters, we aimed to see which model had higher performance and to examine the impact of input factors on outputs. Fig. 5 depicts the computed deviations for all data. As we review the figures, we notice that Model 2 can predict with higher accuracy than Model 1 for U_o and ΔP_1 values. When the same evaluation is made for ΔP_2 and C_{sum} values, we see that Model 1 has a higher estimated performance than Model 2. According to the obtained results, the pumping powers of the inner and annulus sides of the HEX are found as unnecessary input parameters of ANN analyses because the prediction rates of Group 1 input parameters seem satisfactory as shown in Table 1. Normally, it is expected that predictability is supposed to increase as input parameters increase. However, there is a reality that noise issues in the analyses sometimes can occur due to unnecessary input parameters affecting the learning algorithm negatively. From this point of view, the noise issue begins in Fig. 5b and continues to Fig. 5d. Group 2, having pumping powers that involve pressure drops in their formulas, has less predictability than Group 1, but it is supposed to have contrary performance.

Finally, further discussions, figures, and tables on the HT, PD, and cost analysis of the determination of optimum velocity have not

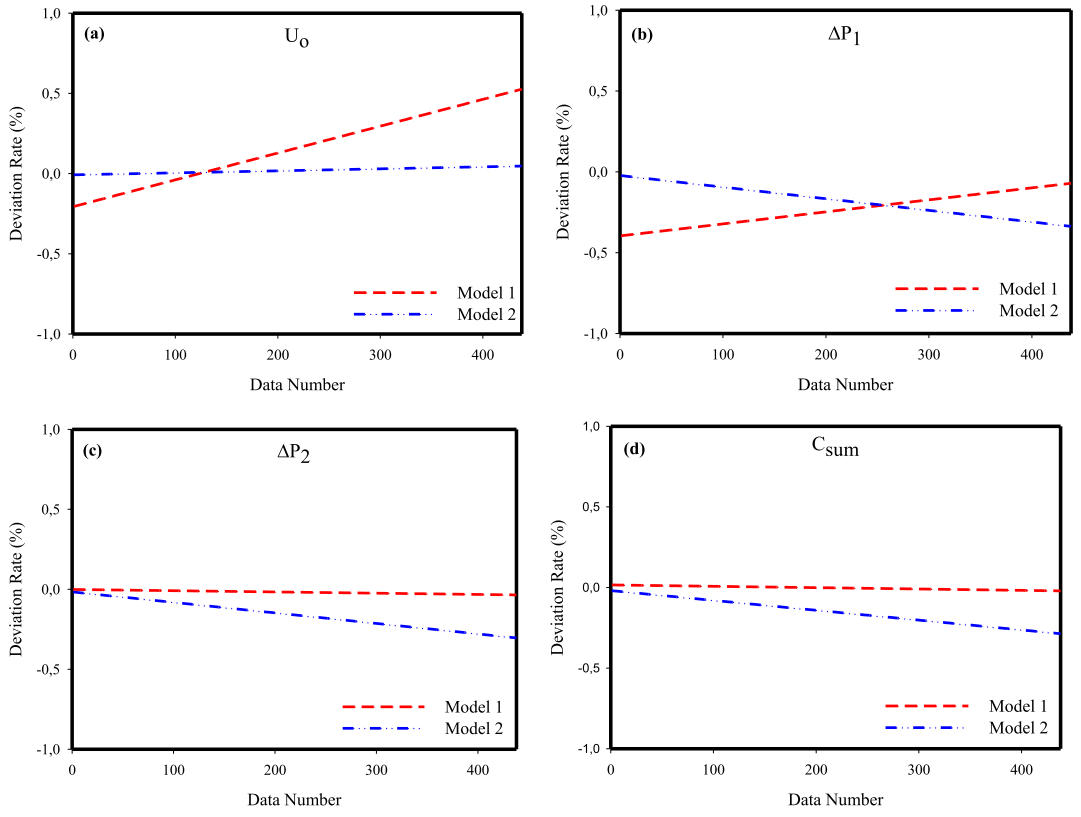

Fig. 5. Deviation rates for the ANN models.

Table 1
Performance parameters for the ANN models.

	Model 1			Model 2		
	MSE	Deviation	R	MSE	Deviation	R
$\mathbf{U_o}$	2.19E-03	0.16	0.98197	1.11E-04	0.02	0.98453
$\mathbf{\Delta P_1}$	9.14E-03	−0.23		1.90E-04	−0.18	
$\mathbf{\Delta P_2}$	2.54E-04	−0.02		6.44E-02	−0.16	
$\mathbf{C_{sum}}$	1.93E-04	−0.003		5.59E-02	−0.15	

been provided in the current study. Due to page limitations, they exist in Refs. [26,27]. Only ANN results are presented in the current work.

5. Conclusion

Tube-in-tube HEXs are the unsophisticated shape of HEXs employed in the industry. Since they are affordable to possess, and they require low-cost service, small and medium-sized enterprises usually prefer them. However, they reserve a remarkable place yet have low efficiency in comparison to others. In the current work, the temperatures at the tube and annulus side of the HEXs have been found identical. Because the fluid flow rate at the annulus side has a fixed value, the heat load is equal to all investigated fluids. Two dissimilar and important physical characteristics happen in this type of HEX: fluid flow in tubes and HT between the fluid and annulus wall. Thus, improving the mechanisms occurring through those characteristics enhances HT. Augmenting the thermophysical specifications of the tested fluids having nanoparticles to enable a preferable overall HTC can be favored to improve HT. In the current situation, considering both annual investment and operation expenditures, determining optimal velocities for the studied fluids given the most economical working conditions have been beneficial in data sets of ANN analyses.

In the present work, two unique ANN models with various input factors are generated, and U_o, ΔP_1, ΔP_2, and C_{sum} values are estimated. ρ, n_p, k_1, Re_1, f_i, Re_2, f_o, n_s, P_1 and P_2 values have been described in the input layer of the first model, while P_1 and P_2 parameters have been extracted in the second model. There are 15 neurons in the hidden layer of developed MLP networks, and the Levenberg-Marquardt procedure is evaluated as the training algorithm. About 70% of the data employed in the ANN models designed with a total of 438 data sets were classified for model training, 15% for validation, and 15% for the testing stage. Overall HT coefficient, tube, and annulus side pressure drop, and overall cost have been estimated with the deviations of 0.16%, −0.23%, −0.02%, and −0.003% via Model 1, 0.02%, −0.18%, −0.16%, and −0.15% via Model 2. The noise issue has also been investigated using unnecessary input parameters. The ANN model developed from the present work may be widened by adjusting it to other fluids along with HEX types, provided that the outcomes are verified by prevalent references in the open sources.

Author statement

Andaç Batur Çolak: Conceptualization, Software, Writing – original draft.
Özgen Açıkgöz: Investigation, data curation, methodology.
Hatice Mercan: Review.
Ahmet Selim Dalkılıç: Supervision, project administration.
Somchai Wongwises: Writing - review & editing, funding acquisition.

Declaration of competing interest

The authors declare that they have no known competing financial interests or personal relationships that could have appeared to influence the work reported in this paper.

Data availability

Data will be made available on request.

Acknowledgment

The fourth author acknowledges the Visiting Professorship from KMUTT. The fifth author acknowledges the National Science and Technology Development Agency (NSTDA) under the “Research Chair Grant”, and the Thailand Science Research and Innovation (TSRI) under Fundamental Fund 2022.

References

[1] M. Mohanraj, S. Jayaraj, C. Muraleedharan, Applications of artificial neural networks for thermal analysis of heat exchangers–a review, Int. J. Therm. Sci. 90 (2015) 150–172.
[2] R.M. Devi, P. Murugesan, M. Venkatesan, P. Keerthika, K. Sudha, J.C. Kannan, P. Suresh, Development of MLP-ANN model to predict the Nusselt number of plain swirl tapes fixed in a counter flow heat exchanger, Mater. Today Proc. 46 (2021) 8854–8857.
[3] K. Sharifi, M. Sabeti, M. Rafiei, A.H. Mohammadi, A. Ghaffari, M.H. Asl, H. Yousefi, A good contribution of computational fluid dynamics (CFD) and GA-ANN methods to find the best type of helical wire inserted tube in heat exchangers, Int. J. Therm. Sci. 154 (2020), 106398.

[4] J.D. Moya-Rico, A.E. Molina, J.F. Belmonte, J.C. Tendero, J.A. Almendros-Ibanez, Characterization of a triple concentric-tube heat exchanger with corrugated tubes using Artificial Neural Networks (ANN), Appl. Therm. Eng. 147 (2019) 1036–1046.
[5] T.N. Verma, P. Nashine, D.V. Singh, T.S. Singh, D. Panwar, ANN: prediction of an experimental heat transfer analysis of concentric tube heat exchanger with corrugated inner tubes, Appl. Therm. Eng. 120 (2017) 219–227.
[6] M. Hojjat, Nanofluids as coolant in a shell and tube heat exchanger: ANN modeling and multi-objective optimization, Appl. Math. Comput. 365 (2020), 124710.
[7] A. Taheri, M.G. Moghadam, M. Mohammadi, M. Passandideh-Fard, M. Sardarabadi, A new design of liquid-cooled heat sink by altering the heat sink heat pipe application: experimental approach and prediction via artificial neural network, Energy Convers. Manag. 206 (2020), 112485.
[8] P. Naphon, S. Wiriyasart, T. Arisariyawong, L. Nakharintr, ANN, numerical and experimental analysis on the jet impingement nanofluids flow and heat transfer characteristics in the micro-channel heat sink, Int. J. Heat Mass Tran. 131 (2019) 329–340.
[9] E. Davoudi, B. Vaferi, Applying artificial neural networks for systematic estimation of degree of fouling in heat exchangers, Chem. Eng. Res. Des. 130 (2018) 138–153.
[10] O. Duran, N. Rodriguez, L.A. Consalter, Neural networks for cost estimation of shell and tube heat exchangers, Expert Syst. Appl. 36 (4) (2009) 7435–7440.
[11] M. Noorbakhsh, S.S.M. Ajarostaghi, M. Zaboli, B. Kiani, Thermal analysis of nanofluids flow in a double pipe heat exchanger with twisted tapes insert in both sides, J. Therm. Anal. Calorim. 147 (2022) 3965–3976.
[12] S.H.H. Karouei, S.S.M. Ajarostaghi, S. Rashidi, E. Hosseinirad, An advanced turbulator with blades and semi-conical section for heat transfer improvement in a helical double tube heat exchanger, J. Cent. South Univ. 28 (2021) 3491–3506.
[13] M. Noorbakhsh, M. Zaboli, S.S.M. Ajarostaghi, Numerical evaluation of the effect of using twisted tapes as turbulator with various geometries in both sides of a double-pipe heat exchanger, J. Therm. Anal. Calorim. 140 (2020) 1341–1353.
[14] S.H.H. Karouei, S.S.M. Ajarostaghi, M. Gorji-Bandpy, S.R.H. Fard, Laminar heat transfer and fluid flow of two various hybrid nanofluids in a helical double-pipe heat exchanger equipped with an innovative curved conical turbulator, J. Therm. Anal. Calorim. 143 (2021) 1455–1466.
[15] S.H.H. Karouei, S.S.M. Ajarostaghi, Influence of a curved conical turbulator on heat transfer augmentation in a helical double-pipe heat exchanger, Heat Transfer 50 (2020) 1872–1894.
[16] M. Sridharan, Application of fuzzy logic expert system in predicting cold and hot fluid outlet temperature of counter-flow double-pipe heat exchanger, in: Advanced Analytic and Control Techniques for Thermal Systems with Heat Exchangers, Academic Press, 2020, pp. 307–323.
[17] E. Wallhäußer, M.A. Hussein, T. Becker, Detection methods of fouling in heat exchangers in the food industry, Food Control 27 (1) (2012) 1–10.
[18] M. Bahiraei, H.K. Salmi, M.R. Safaei, Effect of employing a new biological nanofluid containing functionalized graphene nanoplatelets on thermal and hydraulic characteristics of a spiral heat exchanger, Energy Convers. Manag. 180 (2019) 72–82.
[19] S.M. Hosseini, M.R. Safaei, P. Estellé, S.H. Jafarnia, Heat transfer of water-based carbon nanotube nanofluids in the shell and tube cooling heat exchangers of the gasoline product of the residue fluid catalytic cracking unit, J. Therm. Anal. Calorim. 140 (2020) 351–362.
[20] N. Pandey, K. Murugesan, H.R. Thomas, Optimization of ground heat exchangers for space heating and cooling applications using Taguchi method and utility concept, Appl. Energy 190 (2017) 421–438.
[21] D. Ndiaye, Transient model of a refrigerant-to-water helically coiled tube-in-tube heat exchanger with corrugated inner tube, Appl. Therm. Eng. 112 (2017) 413–423.
[22] J.H. Xie, H.C. Cui, Z.C. Liu, W. Liu, Optimization design of helical micro fin tubes based on exergy destruction minimization principle, Appl. Therm. Eng. 200 (2022), 117640.
[23] N.H. Abu-Hamdeh, A. Alimoradi, Investigation of the effect of the finned coiled wire insert on the heat transfer intensification of circular tube: energy and exergy analysis, Chem. Eng. Process. Process Intensif. 160 (2021), 108245.
[24] Z.X. Li, F.L. Renault, A.O.C. Gómez, M.M. Sarafraz, H. Khan, M.R. Safaei, E.P. Bandarra Filho, Nanofluids as secondary fluid in the refrigeration system: experimental data, regression, ANFIS, and NN modeling, Int. J. Heat Mass Tran. 144 (2019), 118635.
[25] A. Alimoradi, F. Veysi, Prediction of heat transfer coefficients of shell and coiled tube heat exchangers using numerical method and experimental validation, Int. J. Therm. Sci. 107 (2016) 196–208.
[26] A.S. Dalkılıç, O. Acikgoz, M.A. Gümüş, S. Wongwises, Determination of optimum velocity for various nanofluids flowing in a double-pipe heat exchanger, Heat Tran. Eng. 38 (1) (2017) 11–25.
[27] A.S. Dalkılıç, H. Mercan, G. Özçelik, S. Wongwises, Optimization of the finned double-pipe heat exchanger using nanofluids as working fluids, J. Therm. Anal. Calorim. 143 (2) (2021) 859–878.
[28] O.F. Genceli, Isı Değiştiricileri, İstanbul: Birsen Yayınevi, 1999.
[29] M. Ledinegg, Dampferzeugung, Dampfkessel, Feuerungen: Theorie, Konstruktion, Betrieb, Springer-Verlag, 2013.
[30] H. Hausen, Neue Gleichungen für die Wȯrmeübertragung bei freier und erzwungener Strmung, Allg. Wȯrmetechnik. 9 (1959) 75–79.
[31] F.P. Incropera, D.P. DeWitt, T.L. Bergman, A.S. Lavine, Fundamentals of Heat and Mass Transfer, vol. 6, Wiley, New York, 1996, p. 116.
[32] O. Frank, Simplified design procedures for tubular exchangers I. Practical aspects of heat transfer, Chem. Eng. Prog. Tech. Manual (Am. Inst. Chem. Eng.) (1978).
[33] Y.A. Cengel, J.M. Cımbala, Fluid Mechanics: Fundamentals and Applications, McGraw-Hill Education, New York, 2013.
[34] M. Afrand, K.N. Najafabadi, N. Sina, M.R. Safaei, A.Sh Kherbeet, S. Wongwises, M. Dahari, Prediction of dynamic viscosity of a hybrid nano-lubricant by an optimal artificial neural network, Int. Commun. Heat Mass Tran. 76 (2016) 209–214.
[35] A. Canakci, S. Ozsahin, T. Varol, Modeling the influence of a process control agent on the properties of metal matrix composite powders using artificial neural networks, Powder Technol. 228 (2012) 26–35.
[36] T. Güzel, A.B. Çolak, An experimental study on artificial intelligence-based prediction of capacitance-voltage parameters of polymer-interface 6H-SiC/MEH-PPV/Al Schottky diodes, Phys. Status Solidi 219 (5) (2022), 2100821.
[37] E. Ahmadloo, S. Azizi, Prediction of thermal conductivity of various nanofluids using artificial neural network, Int. Commun. Heat Mass Tran. 74 (2016) 69–75.
[38] A.B. A Çolak, An experimental study on the comparative analysis of the effect of the number of data on the error rates of artificial neural networks, Int. J. Energy Res. 45 (1) (2021) 478–500.
[39] F. Esmaeilzadeh, A.S. Teja, A. Bakhtyari, The thermal conductivity, viscosity, and cloud points of bentonite nanofluids with n-pentadecane as the base fluid, J. Mol. Liq. 300 (2020), 112307.
[40] A.B. Çolak, O. Yıldız, M. Bayrak, B.S. Tezekici, Experimental study for predicting the specific heat of water based Cu-Al_2O_3 hybrid nanofluid using artificial neural network and proposing new correlation, Int. J. Energy Res. 44 (9) (2020) 7198–7215.
[41] S.H. Rostamian, M. Biglari, S. Saedodin, M.H. Esfe, An inspection of thermal conductivity of CuO-SWCNTs hybrid nanofluid versus temperature and concentration using experimental data, ANN modeling and new correlation, J. Mol. Liq. 231 (2017) 364–369.
[42] A.B. Çolak, Experimental analysis with specific heat of water based zirconium oxide nanofluid on the effect of training algorithm on predictive performance of artificial neural network, Heat Tran. Res. 52 (7) (2021) 67–93.
[43] A. Ali, A. Abdulrahman, S. Garg, K. Maqsood, G. Murshid, Application of artificial neural networks (ANN) for vapor-liquid-solid equilibrium prediction for CH_4-CO_2 binary mixture, Greenh. Gases: Sci. Technol. 9 (1) (2019) 67–78.
[44] A.A.A.A. Alrashed, A. Karimipour, S.A. Bagherzadeh, M.R. Safaei, M. Afrand, Electro- and thermophysical properties of water-based nanofluids containing copper ferrite nanoparticles coated with silica: experimental data, modeling through enhanced ANN and curve fitting, Int. J. Heat Mass Tran. 127 (2018) 925–935.
[45] M. Vafaei, M. Afrand, N. Sina, R. Kalbasi, F. Sourani, H. Teimouri, Evaluation of thermal conductivity of MgO-MWCNTs/EG hybrid nanofluids based on experimental data by selecting optimal artificial neural networks, Phys. E Low-dimens. Syst. Nanostruct. 85 (2017) 90–96.
[46] A. Akhgar, D. Toghraie, N. Sina, M. Afrand, Developing dissimilar artificial neural networks (ANNs) to prediction the thermal conductivity of MWCNT-TiO_2/Water-ethylene glycol hybrid nanofluid, Powder Technol. 355 (2019) 602–610.

[47] A.B. Çolak, A novel comparative investigation of the effect of the number of neurons on the predictive performance of the artificial neural network: an experimental study on the thermal conductivity of ZrO_2 nanofluid, Int. J. Energy Res. 45 (13) (2021) 18944–18956.
[48] S. Öcal, M. Gökçek, A.B. Çolak, M. Korkanç, A comprehensive and comparative experimental analysis on thermal conductivity of TiO_2-$CaCO_3$/water hybrid nanofluid: proposing new correlation and artificial neural network optimization, Heat Tran. Res. 52 (17) (2021).
[49] E. Bas, V.R. Uslub, E. Egrioglu, Robust learning algorithm for multiplicative neuron model artificial neural networks, Expert Syst. Appl. 56 (2016) 80–88.
[50] M. Bahiraei, S. Heshmatian, H. Moayedi, Artificial intelligence in the field of nanofluids: a review on applications and potential future directions, Powder Technol. 353 (2019) 276–301.
[51] S. Delfani, M. Esmaeili, M. Karami, Application of artificial neural network for performance prediction of a nanofluid-based direct absorption solar collector, Sustain. Energy Technol. Assessments 36 (2019), 100559.
[52] A.H.A. Al-Waeli, K. Sopian, J.H. Yousif, H.A. Kazem, J. Boland, M.T. Chaichan, Artificial neural network modeling and analysis of photovoltaic/thermal system based on the experimental study, Energy Convers. Manag. 186 (2019) 368–379.
[53] E. Ahmadloo, S. Azizi, Prediction of thermal conductivity of various nanofluids using artificial neural network, Int. Commun. Heat Mass Tran. 74 (2016) 69–75.
[54] M. Afrand, D. Toghraie, N. Sina, Experimental study on thermal conductivity of water-based Fe3O4 nanofluid: development of a new correlation and modeled by artificial neural network, Int. Commun. Heat Mass Tran. 75 (2016) 262–269.
[55] P. Naphon, S. Wiriyasart, T. Arisariyawong, Artificial neural network analysis the pulsating Nusselt number and friction factor of TiO2/water nanofluids in the spirally coiled tube with magnetic field, Int. J. Heat Mass Tran. 118 (2018) 1152–1159.
[56] E. Aylı, Modeling of mixed convection in an enclosure using multiple regression, artificial neural network, and adaptive neuro-fuzzy interface system models, Proc. IME C J. Mech. Eng. Sci. 234 (2020) 3078–3093.